Recurrence plots of experimental data: To embed or not to embed?

Joseph S. Iwanski and Elizabeth Bradley

Citation: Chaos **8**, 861 (1998); doi: 10.1063/1.166372
View online: http://dx.doi.org/10.1063/1.166372
View Table of Contents: http://scitation.aip.org/content/aip/journal/chaos/8/4?ver=pdfcov
Published by the AIP Publishing

Recurrence plots of experimental data: To embed or not to embed?

Joseph S. Iwanski
Department of Applied Mathematics, University of Colorado, Boulder, Colorado 80309-0526

Elizabeth Bradley[a)]
Department of Computer Science, University of Colorado, Boulder, Colorado 80309-0430

(Received 13 March 1998; accepted for publication 17 August 1998)

A recurrence plot is a visualization tool for analyzing experimental data. These plots often reveal correlations in the data that are not easily detected in the original time series. Existing recurrence plot analysis techniques, which are primarily application oriented and completely quantitative, require that the time-series data first be embedded in a high-dimensional space, where the embedding dimension d_E is dictated by the dimension d of the data set, with $d_E \geqslant 2d+1$. One such set of recurrence plot analysis tools, recurrence quantification analysis, is particularly useful in finding locations in the data where the underlying dynamics change. We have found that for certain low-dimensional systems the same results can be obtained with no embedding. © *1998 American Institute of Physics.* [S1054-1500(98)00604-1]

In general, time-series analysis methods begin with—or at least include—delay-coordinate embedding, a well-established means of reconstructing the hidden dynamics of the system that generated the time series. If the embedding is done correctly, the theorems involved guarantee that certain properties of the original system, known as dynamical invariants, are preserved in the embedded, or reconstruction, space. This is an extremely powerful correspondence, implying that many conclusions drawn from the reconstruction-space dynamics are also true of the real, underlying dynamics. There are, of course, some important caveats; one of the most limiting is that correct embeddings are not easy to construct. Methods in the time-series analysis literature use a variety of heuristics to solve the (significant) problems that are inherent in this process, and the resulting algorithms are often computationally expensive. Time-series analysis methods that do not require embedding are, therefore, extremely desirable. We present evidence suggesting that, for low-dimensional systems, recurrence plots are such a method. Our conclusion is twofold. First, when using current recurrence-plot analysis methods on these types of systems, one need not embed the data. Second, we note that better methods of recurrence plot analysis are needed, methods that take into account the structural and qualitative aspects of these fascinating plots. This work represents a first step towards this goal.

I. INTRODUCTION

First introduced in a 1987 paper by Eckmann, Kamphorst, and Ruelle,[1] the recurrence plot (RP) is an analysis tool for experimental time-series data. A RP is a two-dimensional representation of a single trajectory. The time series spans both ordinate and abscissa, and each point (i,j) on the plane is shaded according to the distance between the two corresponding trajectory points y_i and y_j. [In an unthresholded RP (UTRP), the pixel lying at (i,j) is grey-shaded according to the distance; in a thresholded RP (TRP) the pixel lying at (i,j) is black if the distance falls within a specified threshold corridor and white otherwise. For instance, if the 117th point on the trajectory is 14 distance units away from the 9435th point, the pixel lying at (117, 9435) on the RP will be plotted with the grey shade that corresponds to a spacing of 14. [Point (9435, 117) will be shaded similarly. As originally conceived, however, RPs are not necessarily symmetric.[1]] Figure 1 shows UTRPs generated from two very different data sets: a time series derived by sampling the function $\sin t$ and a time series from the well-known Lorenz system. The grey shades on these plots range from dark for very small spacings to light for large interpoint distances, as shown on the calibration bars in the figure. With this in mind, the sine-wave RPs are relatively easy to understand; each of the ''blocks'' simply represents half a period of the signal.] [Recall that the shading of the point (w,v) on this plot reflects the distance between $\sin w$ and $\sin v$; if $w-v=\pi/2$, for example, that distance is large.] The lower RPs in the figure, generated from a chaotic data set, are far more complicated, although they too have blocklike structures resembling what might be expected from a periodic signal. This signal, though, is not periodic, so the repeated structural elements in the plot beg an explanation.

Recurrence plots are intricate and visually appealing. They are also useful for finding hidden correlations in highly complicated data. Moreover, because they make no demands on the stationarity of a data set, RPs are particularly useful in the analysis of systems whose dynamics may be changing. Although the literature in this area is not extensive, the use of recurrence plots in time-series analysis has become more common in recent years, particularly in the area of physiology. Webber and Zbilut,[2] for instance, used recurrence plot analysis to discern between ''quiet'' and ''active'' breathing in laboratory rats, and Kaluzny and Tarnecki[3] used RPs to

[a)]Electronic mail: lizb@cs.colorado.edu

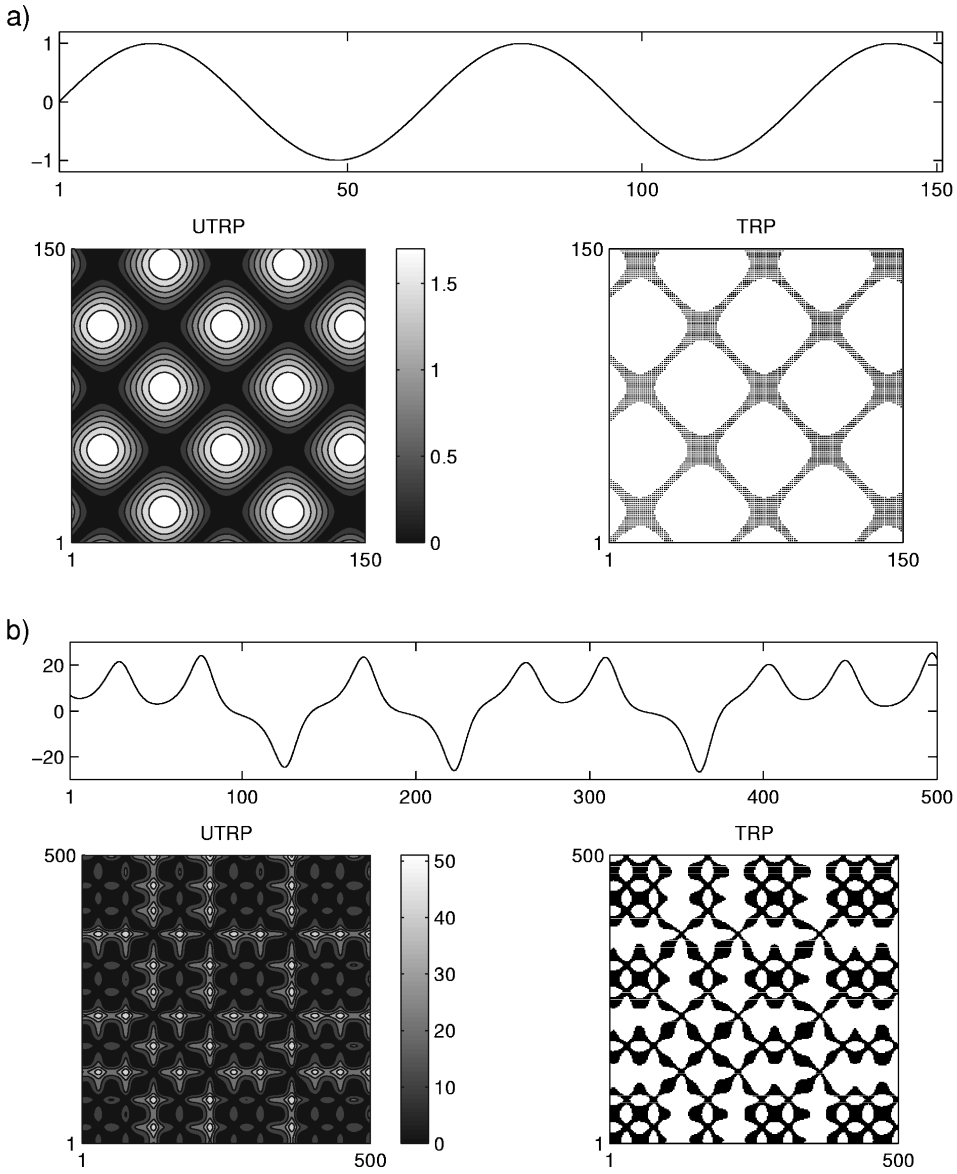

FIG. 1. Recurrence plots: (a) a sine-wave signal and the corresponding recurrence plots and (b) a chaotic signal from the Lorenz system and the corresponding recurrence plots. The shaded plots to the left, known as unthresholded recurrence plots (UTRPs), show the distance relationships between all points in the signal via a gray-scale map. The black and white plots to the right are called thresholded recurrence plots (TRPs) because they highlight only those points that fall within a prescribed distance range. In (a), for example, this range of distances, called a threshold corridor, is [0,0.25]; in (b) the threshold corridor is [0,5.0]. One can see the TRP patterns in the UTRPs by careful examination of the UTRP calibration bars for the given threshold corridor values.

study neuronal spike trains in cats. In mathematical problems, RPs have been used primarily to identify transition points in nonstationary data sets. Trulla *et al.*,[4] for instance, analyzed the dynamics of the logistic equation, varying the driving parameter smoothly and leading the time series between chaotic and periodic regimes. They concluded that RP analysis compares favorably to classical statistical approaches as a means for analyzing chaotic data, particularly in the detection of bifurcations. Very recently, Casdagli[5] used RPs to characterize time series generated by dynamical systems driven by slowly varying external forces.

Our study of recurrence plots has been motivated by the desire to give meaning to the fascinating structures that they exhibit. Previous work in this area is primarily application oriented and completely quantitative. We wish, rather, to extend, formalize, and systematize recurrence plot analysis in a meaningful way that is based both in theory and experiment and that targets both quantitative and qualitative properties. An important consequence of such a formalization is the power that it would lend to the RP as an analysis tool. For example, knowledge of how periodicity and chaos manifest on RPs and how bifurcations affect the geometry and topology of their structure would allow us to use these plots as a means of determining when a system has, for example, moved from a limit cycle to a chaotic regime. The work described in this paper is a first step towards this type of formalization.

While examining several RPs of a particular data set, we noticed that their appearances seemed to remain qualitatively unchanged with varying embedding dimension. Figure 2 il-

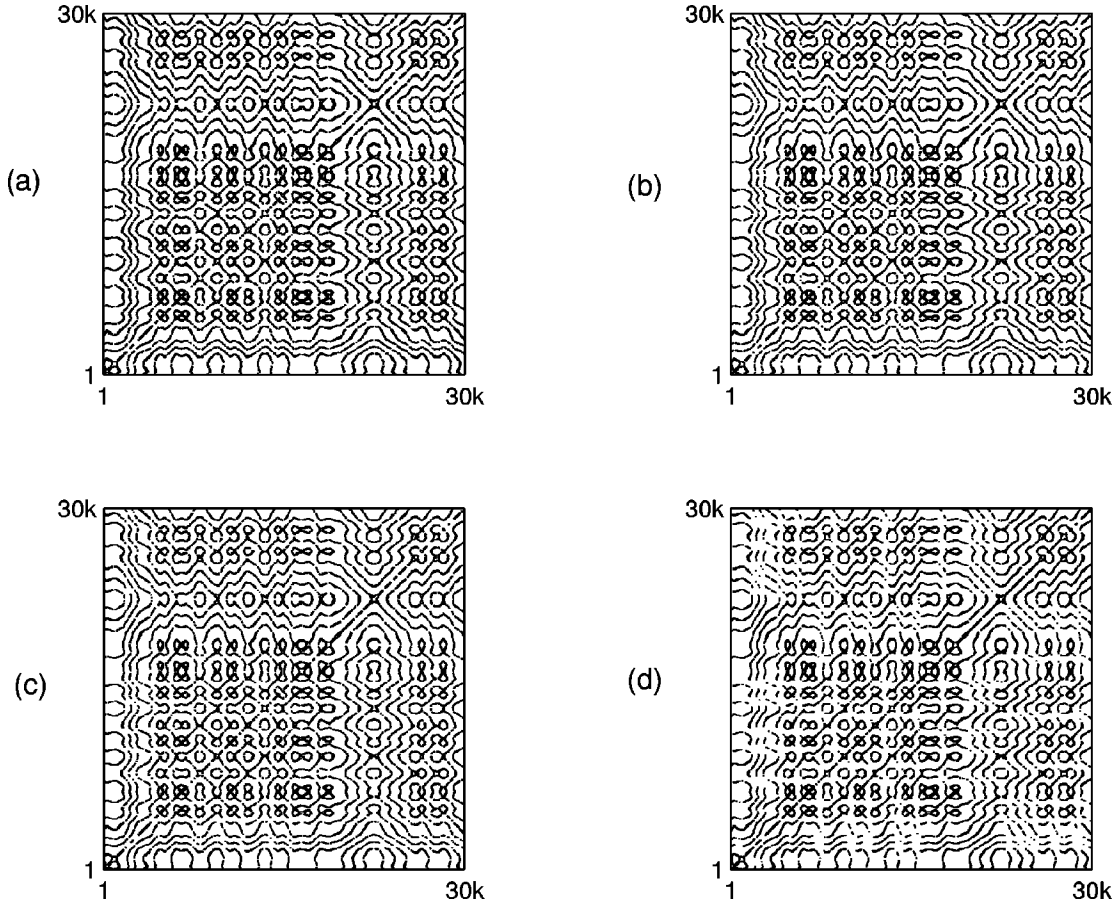

FIG. 2. These four thresholded recurrence plots were generated from a data set gathered from an angle sensor on a parametrically driven pendulum. TRPs (a)–(d) represent embedding dimensions 1–4, respectively, and all four plots have identical threshold corridors and time delay values. Note the striking structural similarity: the only apparent variation is a lightening of the TRP with increasing embedding dimension.

lustrates this for data from an angle sensor on a parametrically driven pendulum. When RPs of other, unrelated data sets also exhibited this type of surprising behavior, the question naturally arose as to whether the quantitative aspects of recurrence plots were independent of the embedding dimension as well. In this paper, we present a suite of numerical calculations on simulated and experimental data sets that explore this question. Specifically, we demonstrate that the recurrence quantification analysis (RQA) of Ref. 4 appears not to depend on the embedding dimension if the data are relatively low-dimensional ($d \leqslant 3$). Analytic justification of this result is a current focus of our effort and the topic of a forthcoming paper.

These results suggest that recurrence plots are more powerful than was previously believed. In all four of the studies mentioned in the related work paragraph above, for example, the data were first embedded in R^{d_E} for some $d_E \geqslant 1$, using the familiar method of delay coordinates.[6] Contrary to current time-series analysis arcana, however, our evidence suggests that d_E need only be equal to one if the data are to be analyzed with RQA. This means that no embedding need be done.

II. RPs AND RECURRENCE QUANTIFICATION ANALYSIS

In this section, we briefly outline some of the basic features of RPs and describe how one generates a RP of an experimental data set. The standard first step in this procedure is to reconstruct the dynamics by embedding the one-dimensional time series in d_E-dimensional reconstruction space using the method of delay coordinates. Given a system whose topological dimension is d, the sampling of a single state variable is equivalent to projecting the d-dimensional phase-space dynamics down onto one axis. Loosely speaking, embedding is akin to ''unfolding'' those dynamics, albeit on different axes. The Takens theorem guarantees that the reconstructed dynamics, if properly embedded, is equivalent to the dynamics of the true, underlying system in the sense that their dynamical invariants, such as generalized dimensions and the Lyapunov spectrum, for example, are identical.[7,8] The process of constructing a correct embedding is the subject of a large body of literature and numerous heuristic algorithms and arguments; Abarbanel's recent text[9] gives a good summary of this extremely active field. The basic problem is to choose two parameters—the delay and the reconstruction-space dimension—that guarantee an *embedding* of the data. (Used precisely, the term embedding refers to a one-to-one map that also preserves tangent directions.) This process is difficult because, in general, one does not have prior knowledge of d's correct value; all one has is a one-dimensional time series and from this one would like to learn as much as possible about the system that generated the signal. Given a trajectory in the embedded space, finally,

one constructs a RP by computing the distance between every pair of points (y_i, y_j) using an appropriate norm and then shading each pixel (i,j) according to that distance.

A. Delay coordinate embedding

To reconstruct the dynamics, one begins with experimental data consisting of a time series:

$$\{x_1, x_2, \ldots, x_N\}.$$

Delay-coordinate reconstruction of the unobserved and possibly multi-dimensional phase-space dynamics from this single observable x is governed by two parameters, embedding dimension d_E and time delay τ. The resultant trajectory in R^{d_E} is

$$\{y_1, y_2, \ldots, y_m\},$$

where $m = N - (d_E - 1)\tau$ and

$$y_k = (x_k, x_{k+\tau}, x_{k+2\tau}, \ldots, x_{k+(d_E-1)\tau})$$

for $k = 1,2,\ldots,m$. Note that using $d_E = 1$ merely returns the original time series; one-dimensional embedding is equivalent to not embedding at all. Proper choice of d_E and τ is critical to this type of phase-space reconstruction and must therefore be done wisely; only ''correct'' values of these two parameters yield embeddings that are guaranteed—by the Takens Theorem[8] and subsequent work by Packard *et al.*[7] and Sauer, Yorke and Casdagli[6]—to be topologically equivalent to the original (unobserved) phase-space dynamics.

There are numerous methods for choosing the embedding dimension and time delay. The formal requirements on the latter are somewhat less stringent; τ must be long enough so that the reconstructed dynamics are ''inflated'' off the main diagonal of the reconstruction space—*with respect to the floating-point arithmetic system that is involved in the calculations*—but not so long that points in the embedded trajectory become uncorrelated. The most widely used approach to estimating such a τ, which we follow in this paper, involves analyzing the data's *average mutual information* function.[10] However, beyond heuristics like average mutual information and loose arguments based on finite-precision arithmetic, it is difficult to say whether one value of time delay is ''good'' or ''bad.'' The time delay is, of course, closely tied to the sampling frequency, in that τ can only be equal to integer multiples of the sampling period. Embedding dimension d_E is harder to determine and its effects on the reconstructed dynamics are more obvious and apparent. If the d_E is too small, projection-induced effects will remain in the reconstructed dynamics, destroying their topological conjugacy to the true dynamics. One of the most common methods for choosing d_E (Ref. 11) is based on the geometry of projection: one adds embedding dimensions, unfolding the dynamics and removing *false near neighbors* (points that are close in m-space but not in $m+1$-space).

If delay-coordinate embedding has been correctly carried out, the dynamical invariants of the true and reconstructed dynamics are identical, so it is natural to assume that the RP of a reconstructed trajectory bears at least some similarity to a RP of the true dynamics. Furthermore, one might expect any properties of the reconstructed trajectory inferred from this RP to hold for the underlying system as well. This is, in fact, the rationale behind the standard procedure of embedding the data before constructing a recurrence plot.

B. Constructing the recurrence plot

Recurrence plots are based upon the mutual distances between points on a trajectory, so the first step in their construction is to choose a norm D. For the work presented here, we use the maximum norm, although in one dimension the maximum norm is, of course, equivalent to the Euclidean p-norm. We chose the maximum norm for ease of implementation and because the maximum distance arising in the recurrence calculations (the difference between the largest and smallest measurements in the time series) is independent of embedding dimension d_E for this particular norm. This means that we can make direct comparisons between RPs generated using different values of d_E without first having to rescale the plots. Using the Euclidean two-norm, on the other hand, interpoint distances increase with embedding dimension simply because length along a new dimension can only contribute to the total distance. It is trivial to show that distance $D(y_i, y_j)$, as measured by Euclidean p-norm or the maximum norm, is nondecreasing with respect to d_E. The point of using the maximum norm was to mitigate this effect.

Next, we define the *recurrence matrix* A as follows:

$$A(i,j) = D(y_i, y_j), 1 \leqslant i,j \leqslant m,$$

$$D(y_i, y_j) = \max_{1 \leqslant k \leqslant d_E} |x_{i+(k-1)\tau} - x_{j+(k-1)\tau}|.$$

We then generate an unthresholded recurrence plot (UTRP) of the time series by plotting matrix A as a contour plot (see Fig. 1). Since current recurrence-plot analysis methods, including the methods defined in Ref. 4, focus on thresholded recurrence plots (TRPs), the next step is to use the UTRP to choose a *threshold corridor*, $[\delta_l, \delta_h]$. This is done by first visually examining the UTRP in order to find interesting structures, and then using the corresponding values from the UTRP colorbar as values for δ_l and δ_h, thus isolating these structures. *Interesting* structures are those whose appearance is best described as being somewhat continuous—resembling an underlying skeleton for the rest of the UTRP—and that persist for different threshold corridors. For simulated data from the Lorenz and Rössler systems, for example, this procedure is relatively easy. However, for other systems in which such structural organization may not be present we are relegated to the somewhat *ad hoc* procedure of choosing a threshold corridor that represents some percentage of the total range of recurrence distances present in the UTRP. The latter method is what is generally used in the literature. This choice has sweeping effects on the RP and some interesting implications for ''false recurrences:'' [5] points that appear close because the embedding dimension is too low and not because of the underlying dynamics.

The choice of the width of the threshold corridor $[\delta_l, \delta_h]$ is critical; too large a corridor results in saturation of the entire TRP—where every pixel is black—while a corridor

that is too narrow will not be adequately populated with points to support the analyses that follow. Besides being critically important, the selection of threshold corridor is also difficult to systematize in any sensible way. Solutions in the literature are unsatisfying; Webber and Zbilut, without comment, prescribe a threshold corridor corresponding to the lower 10% of the entire distance range present in the corresponding UTRP. Our procedure, which uses corridor boundary values that isolate ''interesting'' structures in the UTRP, is also somewhat unsatisfying, and we are working on developing a better formalization. In the meantime, it is an adequate preliminary approach; for instance, it allowed us to reproduce the results in Ref. 4, even though that paper did not specify a threshold corridor.

The absolute position of the threshold corridor is another important and difficult issue. Our threshold corridor procedure allows us to isolate and examine interesting structures *across the range of recurrence distances*—unlike most existing TRP approaches, which specify threshold corridors of the form $[0,r]$. This is an important advantage, as it allows us to examine recurrence structures comprised of points that are not false near neighbors (FNNs) in reconstruction space. (The process of unfolding the attractor—increasing d_E—effectively eliminates FNNs, points that are neighbors in low-dimensional space due only to projection and not to the underlying dynamics.[11]) In this way we attempt to avoid false recurrences.

Once the threshold corridor has been chosen, it is used to generate a *thresholded recurrence matrix* B:

$$B(i,j)=\begin{cases}1 & \text{if } \delta_l \leqslant D(y_i,y_j) \leqslant \delta_h,\\ 0 & \text{otherwise.}\end{cases}$$

Finally, the TRP is generated by darkening all pixels (i,j) that correspond to nonzero entries in matrix B.

C. Recurrence quantification analysis

Perhaps the key mathematical issue in any attempt to use RPs to analyze experimental data is that of quantifying the structure that appears in the plots. Trulla *et al.*[4] have devised a set of quantifying analyses, collectively called recurrence quantification analysis (RQA), to address this problem. The remainder of this section covers the RQA procedure in detail. We view these techniques as the best-formulated and most-general approach to RP analysis that has been developed to date. However, its lumped statistical nature means that RQA cannot capture many of the spatiotemporal details of the dynamics. Moreover, it appears that the standard first step in this procedure—that of embedding the data—may be unnecessary for low-dimensional systems.

In order to perform RQA on a data set, one first constructs a TRP, choosing a threshold corridor $[\delta_l,\delta_h]$ as described in the previous section, and then uses that TRP to compute five statistical values. The first of these statistics, termed % *recurrence* (REC), is simply the percentage of points on the TRP that are darkened (i.e., those pairs of points whose spacing falls within the corridor). This percentage is precisely what is used to compute the correlation dimension of a data set—Kaplan and Glass,[12] for instance, define correlation dimension as the slope of the linear region in the S-shaped % *recurrence* versus corridor width plot. The RQA, however, stops short of extending the analysis beyond the simple calculation of the percentage of dark points on the plot. The second RQA statistic is called % *determinism* (DET); it measures the percentage of recurrent points in a TRP that are contained in lines parallel to the main diagonal. The main diagonal itself is excluded from these calculations because points there are trivially recurrent. Diagonal lines are included in the analysis if and only if they meet or exceed some prescribed minimum length threshold. Intuitively, DET measures how ''organized'' a TRP is. The third RQA statistic, called *entropy*, is closely related to DET. Entropy (ENT) is calculated by binning the diagonal lines defined in the previous paragraph according to their lengths and using the following formula:

$$ENT=-\sum_{k=1}^{N} P_k \log P_k,$$

where N is the number of bins and P_k is the percentage of all lines that fall into bin k. According to Shannon's information theory,[13] predictability decreases with increasing entropy, so one would expect low values of ENT for TRPs of chaotic data sets, for example. The fourth RQA statistic, termed TREND, measures how quickly a TRP ''pales'' away from the main diagonal. As the name suggests, TREND is intended to detect nonstationarity in the data. The fifth and final RQA statistic is called DIV and is equal to the reciprocal of the longest line length found in the computation of DET, or $1/line_{\max}$. Eckmann, Kamphorst, and Ruelle claim that line lengths on RPs are directly related to the inverse of the largest positive Lyapunov exponent.[1] Short $line_{\max}$ values are therefore indicative of chaotic behavior. In a purely periodic signal—the opposite extreme—lines tend to be very long, so DIV is very small.

The ultimate goal of our work is to improve upon existing methods of RP analysis. The lumped statistics of RQA cannot measure much of the qualitative structure of recurrence plots; in Fig. 3, for example, we show two structurally dissimilar RPs that are almost identical from the standpoint of RQA. Moreover, different parameter choices (minimum line length, corridor, etc.) can have drastic effects on RP structure and RQA results. It is our goal to devise RP analysis methods in which these types of structural, qualitative differences are clearly evident and easy to analyze. The ultimate intent of this line of research is to refine RP analysis techniques to the point where they can be used to gain greater insight into the underlying signals from which the RPs were generated.

III. EXPERIMENTS AND RESULTS

One of the more intriguing—and puzzling—characteristics of recurrence plots of data from low-dimensional systems is the structural stability that they exhibit with increasing embedding dimension. That is, qualitative features that are visible in RPs generated using $d_E=1$ often persist in RPs of the same data embedded in higher dimensions. This may appear counterintuitive, as the delay-coordinate embedding process is designed to ''un-

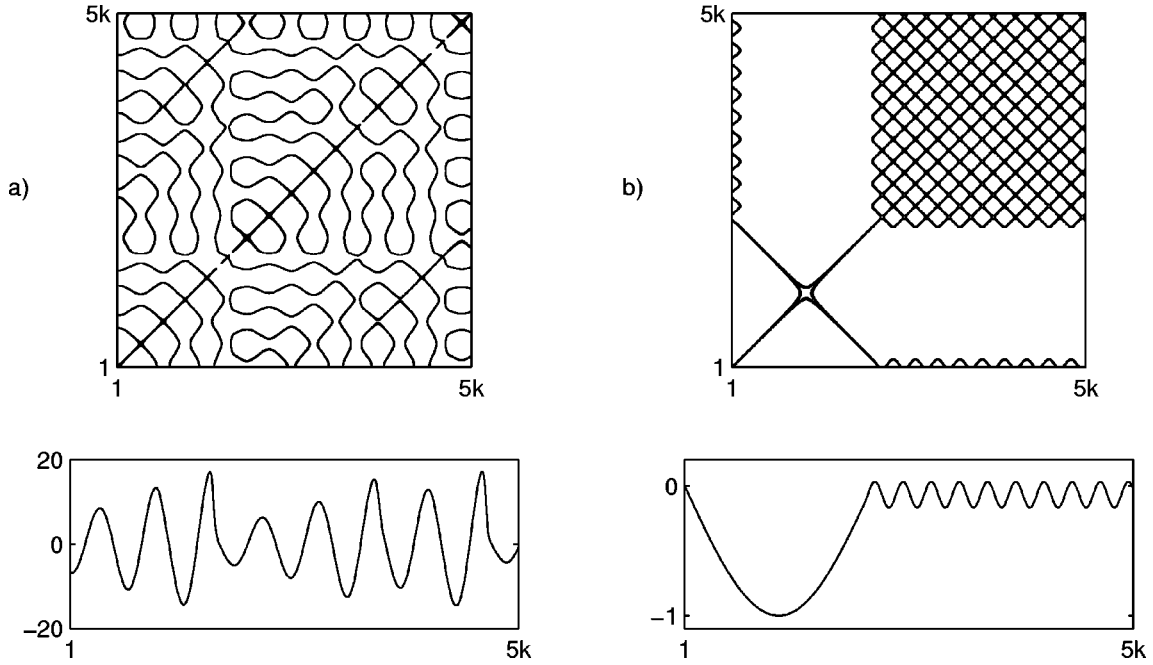

FIG. 3. RQA results on structurally dissimilar TRPs can be almost identical. These two very different TRPs, one (a) from the Rössler system and one (b) a sine-wave signal of varying period, have equal or near-equal values of REC (2.1%) and DET (42.9% for the Rössler data and 45.8% for the varying-period sine wave). Both TRPs were generated from 5000-measurement time series using an embedding dimension of 1 and a minimum line length of 5.

fold'' the underlying dynamics from the one-dimensional time series. Following this line of reasoning, it might be natural to expect that a RP of a formally correct reconstruction ($d_E \geqslant 2d+1$) would be different from RPs of partially unfolded dynamics ($d_E = 1, 2, \ldots, 2d$): that the RP structure would change with embedding dimension until the ''correct'' d_E was reached.

However, this is not generally the case, as is clearly visible in Fig. 2, which shows recurrence plots generated by chaotic data from a parametrically forced pendulum and how those plots change with embedding dimension. This particular system, whose dimension is between 2 and 3, was embedded using the value of time delay as determined by the first local minimum in the average mutual information function, per Ref. 10. Note that the qualitative features of all four TRPs are essentially the same; the major difference is the gradual fading of the TRPs as d_E increases. This is largely due to the fact that an identical threshold corridor was used to generate each plot. As noted in Sec. II B, the distance between any two points on a delay-coordinate reconstructed trajectory is *nondecreasing* with increasing d_E. The threshold corridors in the TRPs in Fig. 2 are all of the form $[\epsilon, r]$, where ϵ is some small number. (We do not use 0 as the lower bound in order to avoid trivial recurrences.) The net effect of a fixed threshold corridor in the face of increasing embedding dimension is that fewer and fewer pairs of points are recurrent, causing the TRP to fade.

The fact that the *qualitative* features of these TRPs are stable with increasing embedding dimension is highly suggestive. In fact, we have noticed this strong pattern of similarity in all of the low-dimensional ($d \leqslant 3$) data sets that we have examined and are currently attempting to understand and justify this analytically. Of particular interest are two aspects of this behavior. First, why does it happen? Recurrence plots expose *distance* relationships in the data—relationships that should (perhaps) change as the dynamics are unfolded by the embedding process. An obvious ansatz is that since the time series really is only one-dimensional, perhaps it makes sense that recurrence patterns present in one-embeddings capture its essential properties. However, such an explanation seems to violate the whole point of the delay-coordinate embedding process, wherein the *multi-dimensional* characteristics of the dynamics are recovered from one-dimensional signals. The second goal of our current research is to work out a formally justifiable and meaningful way to codify the structural characteristics of recurrence plots. Lumped statistical measures, such as those of RQA, are a good starting point, but these methods cannot capture the spatiotemporal details of the dynamics. We are currently investigating various pattern recognition and topological analysis techniques—perhaps focusing on the unstable periodic orbits embedded within the chaotic attractors in the data sets, a set of invariants that can be used to classify the attractor[14]—in order to develop methods that allow sensible and useful structural classification and comparison of RPs.

The experiments reported in the remainder of this section explore these issues in the context of *quantitative* measures of RP structure. Specifically, we investigate how changes in embedding dimension affect the quantitative RP features of two low-dimensional systems, as captured by three of the five RQA statistics. In the first experiment, we duplicate the analyses of Ref. 4—wherein RQA was used to detect dynamical variations in a nonstationary time series derived from the logistic map, embedded in three dimensions—and show that the results are identical if one

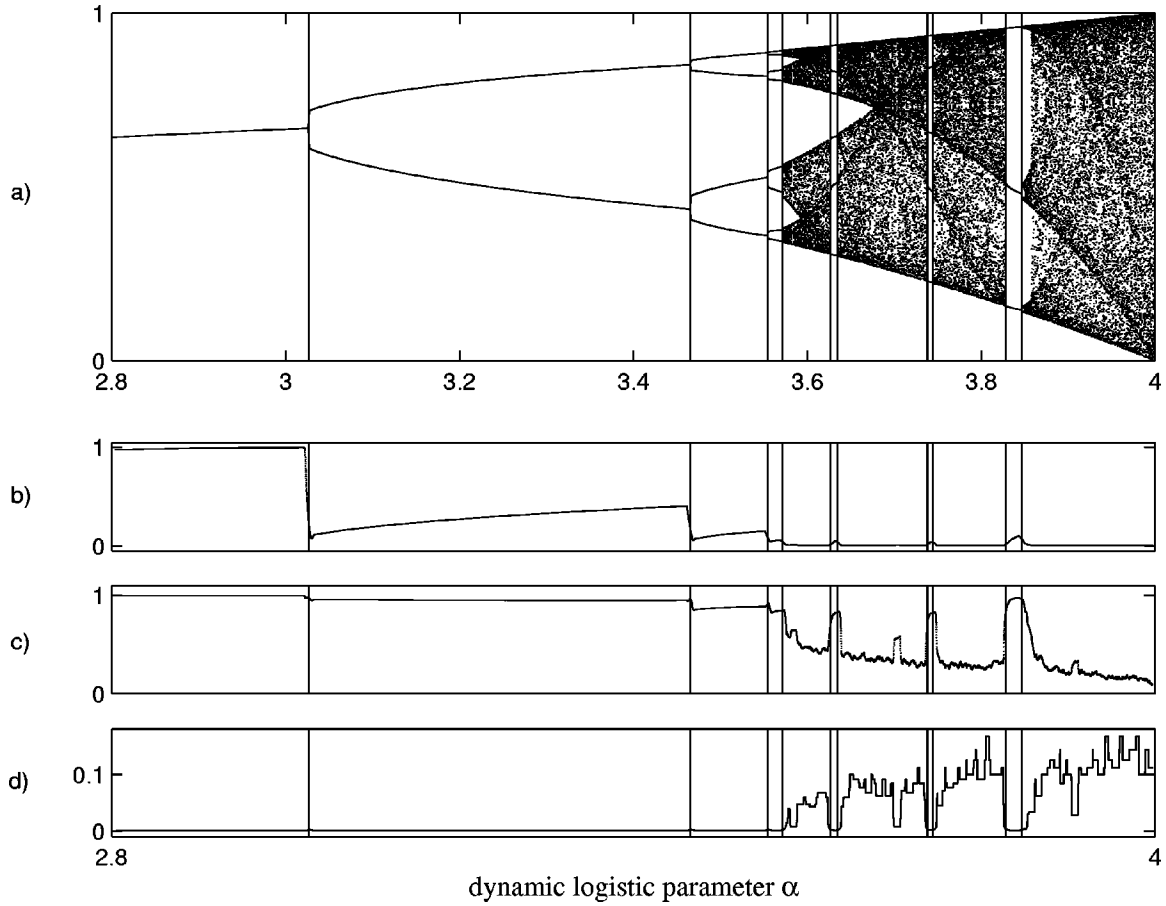

FIG. 4. Using RQA to detect bifurcations: (a) the dynamic logistic map time series, plotted versus parameter α. The vertical lines are drawn at bifurcation points of the signal. This is not the standard bifurcation diagram of the logistic map; here, the transients were not allowed to die out. (b), (c), and (d) show REC, DET, and DIV, respectively, plotted versus parameter α, using embedding dimension $d_E=3$ and time delay $\tau=1$. In all three RQA calculations, threshold corridor was [0,0.0149] and minimum line length was 2. These RQA statistics are clearly effective indicators of the dynamical bifurcations.

uses $d_E=1$, 2, 3, or 4. In the second experiment, we perform a similar RQA analysis on the Lorenz system, again obtaining similar results for different embedding dimensions.

A. Applying RQA to the dynamic logistic map time series

As mentioned in Sec. I, RPs can be used to detect changes in the dynamics of a system. Trulla *et al.*,[4] for instance, used embedding and RQA to recognize bifurcations in the dynamics of the logistic equation. In this section, we duplicate these results *without embedding the data*.

The well-known logistic map is given by the following construction,

$$x_{n+1}=\alpha x_n(1-x_n)$$

for some choice of α, which we will call the dynamic parameter, and some initial condition x_0. When studying this well-known system, one usually fixes the parameter α and iterates the map from x_0, discarding the first few hundred (or thousand) iterates in order to allow any transient behavior to die out. This map exhibits a variety of periodic and chaotic behaviors for dynamic parameter values between $\alpha=2.8$ to 4.0, and the parameter values at which the bifurcations occur are also well known.

In order to show that RQA is an effective method for detecting bifurcations, Trulla *et al.*[4] applied their analyses to a somewhat different logistic map time series—one in which the *transient behavior was not allowed to die out*. They began with dynamic parameter $\alpha=2.8$ and initial condition $x_0=0.6$. After each iteration, they incremented α by 0.00 001 up to $\alpha=4.0$, yielding a nonstationary time series of 120 001 measurements of x. They then embedded the data in three-dimensional space with $\tau=1$, divided the trajectory into 11 920 *epochs* of 800 points, in which epoch $(k+1)$ began ten points farther along the original time series than epoch k, and calculated REC and DET for each epoch in the sequence. [In this formulation, epoch k overlaps with the last 790 points of epoch $(k-1)$ and with the first 790 points of epoch $(k+1)$.] Their main conclusion was that these two RQA statistics were better than classical statistical measurements, such as mean and standard deviation, at distinguishing between periodicity and chaos.

We repeated this analysis using identical parameters and obtained identical results, *independent of embedding dimension*. The results for $d_E=3$ appear in Fig. 4: part (a) shows the signal itself, while (b), (c), and (d) give the REC, DET, and DIV results, respectively, for $d_E=3$ and time delay $\tau=1$. The vertical lines on the figure indicate bifurcation points, as de-

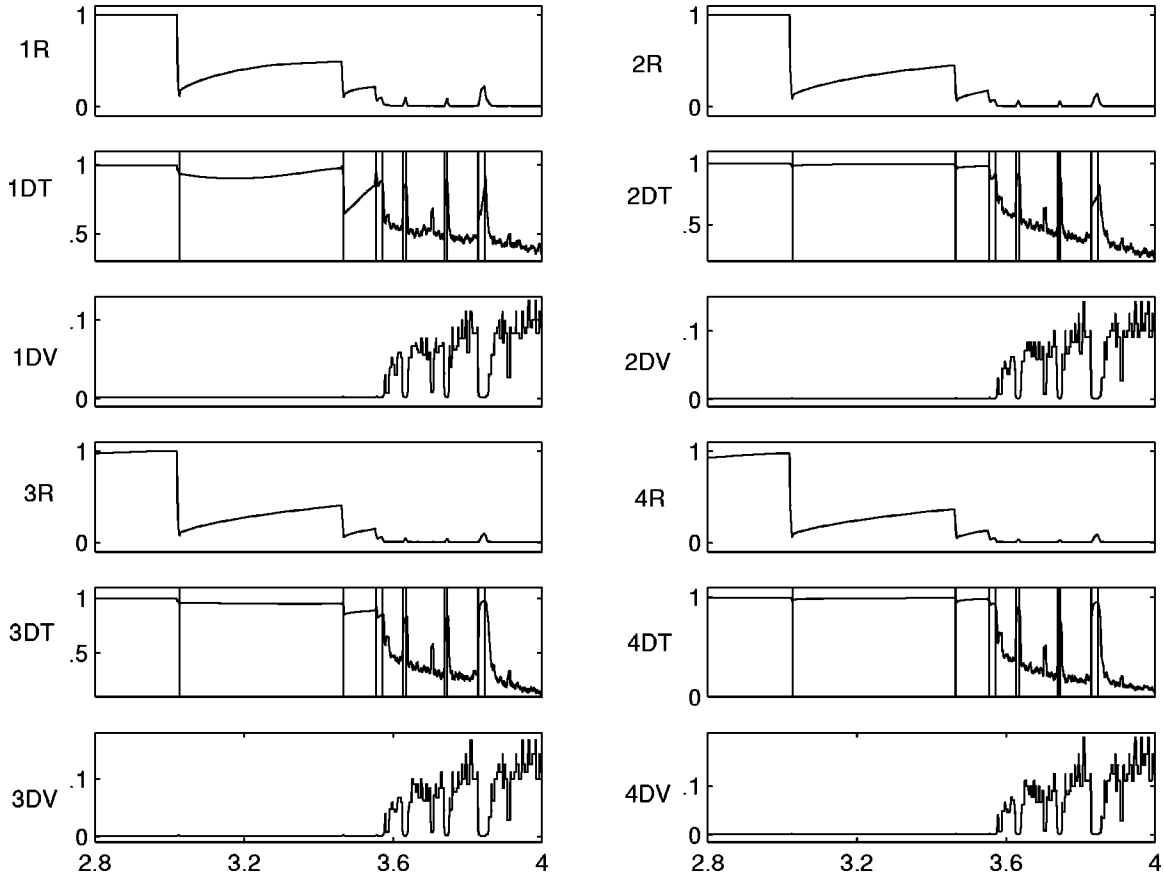

FIG. 5. RQA statistics REC, DET, and DIV computed from the dynamic logistic map data set shown in part (a) of the previous figure. Individual plots are labeled with *R, *DT, or *DV, where number * indicates the embedding dimension and R, DT, and DV denote RQA statistics REC, DET, DIV, respectively. The bifurcation points of the time series are indicated by vertical lines on the DT plots. Note how all three statistics pick up bifurcation points equally well, *regardless of embedding dimension*.

termined by careful examination of the signal. On the whole, the RQA statistics pick these bifurcation points up very nicely. Where the bifurcation involves a transition between periodic and chaotic behavior, there are abrupt changes in all three statistics; in the direction from periodicity to chaos, REC and DET increase and DIV decreases (and vice versa). Changes in all three statistics also accompany bifurcations between different types of periodic orbit—e.g., the two-cycle to four-cycle bifurcation near $\alpha = 3.48$. In DIV, these appear as small spikes, which are somewhat obscured by the scale and the vertical lines. At the period-doubling bifurcations, REC drops sharply because points are suddenly not recurrent with respect to points on the other branch of the orbit. The DET also drops, although not as sharply; the bifurcation leads the dynamics into *another* periodic regime, where the recurrent points are still organized into coherent structures.

In order to explore the role that embedding dimension plays in RQA, we repeated the same analysis with *different* embedding dimensions. The results were virtually identical. Figure 5 illustrates this, showing the same three RQA statistics for the cases $d_E = 1$, 2, 3, and 4. The correspondence is striking: all three RQA statistics pick up the bifurcation points just as well when $d_E = 1$ as when $d_E = 3$, as is apparent from a vertical comparison of the plots in Fig. 5. There are some minor shape differences in the plots, but the bifurcation points are equally distinguishable in all four embeddings. This implies that the results and claims in Ref. 4 may not really require embedding the data.

The logistic map is, of course, fundamentally one-dimensional, so one might naturally expect *any* data analysis results to be independent of d_E. (Trulla *et al.*, do not give any justification for having embedded this time series in R^3.) The next logical step in exploring the effects of embedding dimension on the qualitative and quantitative structure of recurrence plots was to run a similar experiment on data from a higher-dimensional system.

B. Applying RQA to the dynamic Lorenz time series

The results in the previous section suggest that RQA performed on one-embeddings of time-series data is a useful way to detect bifurcations. In this section, we test this hypothesis further by applying RQA to various embeddings of time-series data from the Lorenz system. Specifically, we integrated the Lorenz equations

$$\begin{bmatrix} \dot{x} \\ \dot{y} \\ \dot{z} \end{bmatrix} = \begin{bmatrix} \sigma(y-x) \\ rx-y-xz \\ xy-bz \end{bmatrix} \tag{1}$$

numerically with fourth-order Runge–Kutta and a timestep of 0.01, holding σ and b fixed (10 and 8/3, respectively) and varying r from 28.0 to 268.0, and used the x value as the

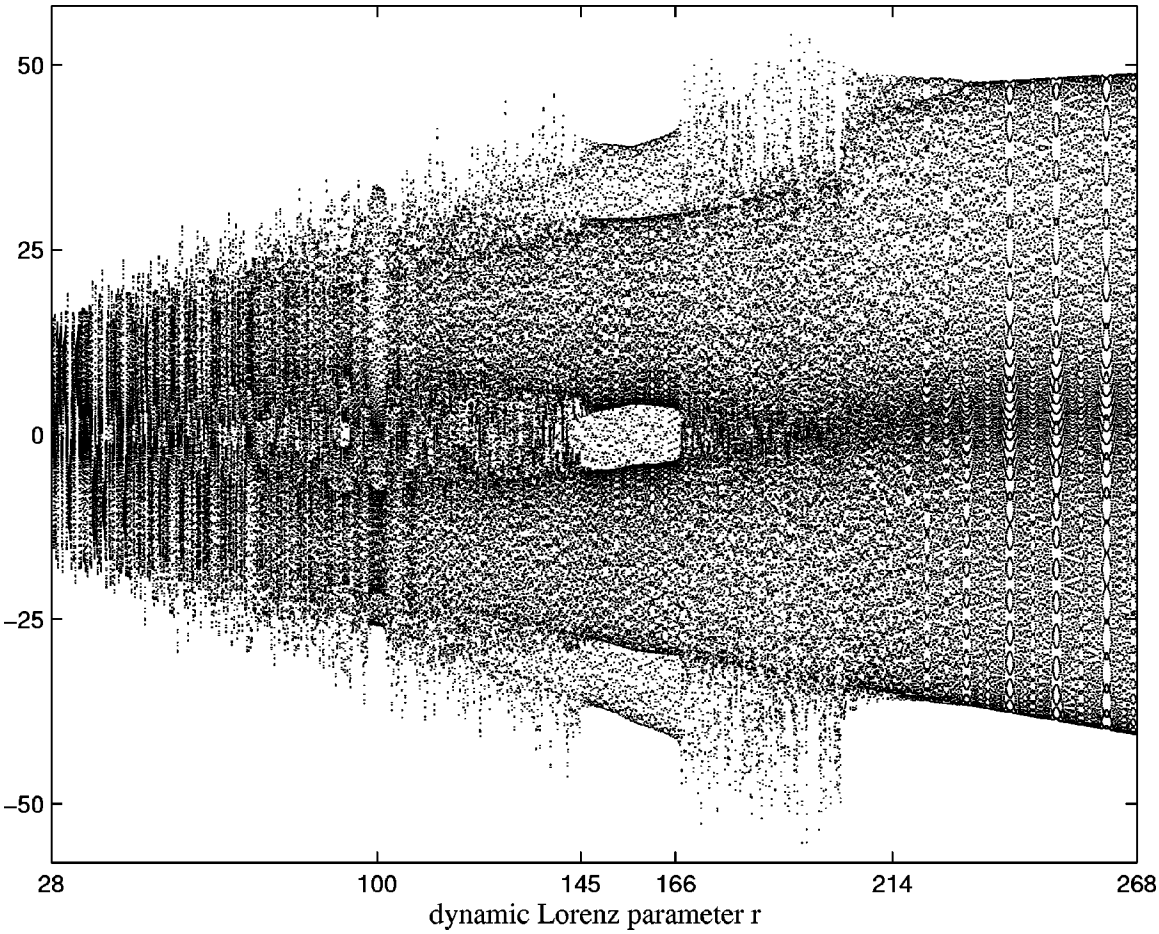

FIG. 6. Dynamic Lorenz time series. This signal was generated from the Lorenz system (1), with fourth-order Runge–Kutta and a timestep of 0.01, by fixing $\sigma = 10.0$, $b = 8/3$, and incrementing the dynamic parameter r from 28.0 to 268.0 by 0.002 at each integration step.

time series. The r-increment was 0.002 per integration step. The signal is shown in Fig. 6. For this particular range of parameter values, the behavior of this system is extremely well studied; see, for example, Refs. 15 and 16. As in the case of the logistic map data of Sec. III A, this time series is somewhat unusual: it includes some amount of transient behavior at each step. One could, of course, allow the transient to die out each time r was incremented before starting to gather time series samples. However, part of the point of this technique is to be able to detect bifurcations as they occur, so an experiment with dynamically changing behavior is an appropriate test case.

The results of RQA on the dynamic Lorenz time series are shown in Fig. 7. The vertical lines on the DT plots identify three of the known periodic windows: $99.524 < r < 100.795$, $145 < r < 166$, and $r > 214.4$. As in the case of the logistic map, the $d_E = 1$, 2, 3, and 4 results are similar.

The DIV is an effective periodic window indicator: all three of the windows correspond to markedly lower values for this RQA statistic, as is clearly visible in Fig. 7 (1DV), (2DV), (3DV), and (4DV). The fluctuation of the values at the beginning of the periodic windows probably stems from the transient nature of the signal; if the transient is slow, the dynamics will require some time to reach the attractor. The flat areas at the very left of the DIV plots—which grow shorter as d_E increases—might also lead one to conclude (mistakenly) that the signal is periodic for r-values just greater than 28. We believe that this anomaly is due in part to the fact that the attractor size changes with r, while we used a single, fixed threshold corridor for the entire signal. (This anomaly did not arise in the dynamic logistic map experiment because the domain of that map is [0,1], independent of α.) A better experiment might be to adapt the threshold corridor in accordance with attractor size; we are currently working out how to do so in a sensible manner. At any rate, it is clear that all four DIV plots are qualitatively quite similar.

The recurrence statistic (REC) is a slightly less-effective bifurcation indicator, but it is still useful, and it too appears to be independent of embedding dimension. The first periodic window (around $r = 100$) is markedly obvious in Fig. 7 (1R), (2R), (3R), and (4R). The second periodic window (between $r = 145$ and $r = 166$) is indicated by a leveling out of REC, but the third one does not leave a strong, well-delineated signature on these plots. Again, this is probably due in large part to the effects of the change in attractor size with parameter r. The similarity of the four plots is the main point we wish to stress here.

The DET results for the dynamic Lorenz signal are shown in Fig. 7 (1DT), (2DT), (3DT), and (4DT). While there is an obvious similarity between the four plots, the (1DT) results give a somewhat less-striking indication of the bifurcations

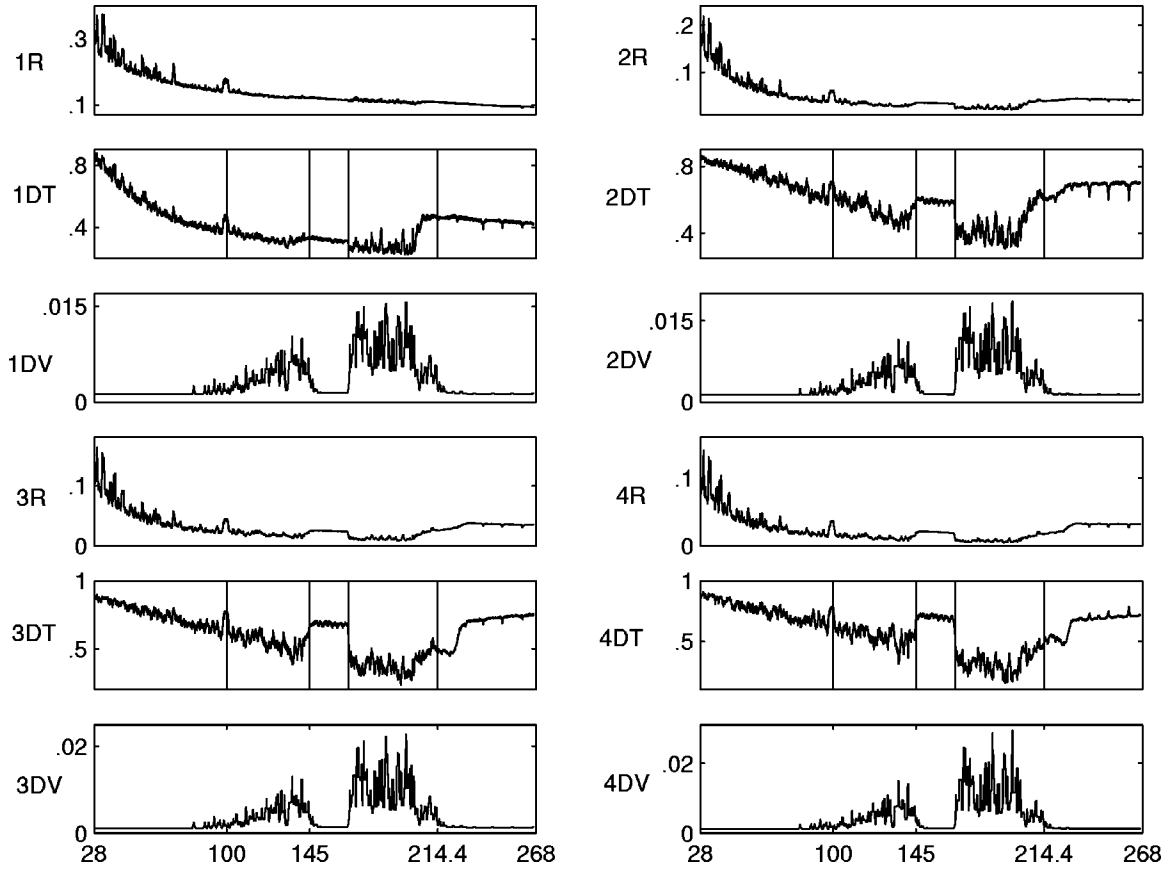

FIG. 7. RQA statistics REC, DET, and DIV computed from the dynamic Lorenz data set shown in the previous figure. Individual plots are labeled with *R, *DT, or *DV, where number * indicates the embedding dimension and R, DT, and DV denote RQA statistics REC, DET, DIV, respectively. Time delay used was $\tau = 0.1$ (10 sample intervals 0.01 each), following Ref. 10. Note how all three statistics pick up bifurcation points equally well, *regardless of embedding dimension*.

than the other plots do. However, the DET indicators are still visible and useful. In particular, the first known periodic window (around $r = 100$) is picked up well by all four plots, as indicated by the spike in the plots at $r = 100$. The $d_E = 2$ and higher DET plots pick out the second known periodic window (between $r = 145$ and 166) much better than the $d_E = 1$ calculations, as indicated by a sharp increase in and leveling out of the DET values in this range. The $d_E = 1$ calculations do give some indication of this window (i.e., the DET values do level out in this range).

Again, these calculations are sensitive to several parameters, particularly the threshold corridor and the minimum line length. In fact, we have found that the minimum line length parameter can drastically alter the results; when we used a minimum line length of 2 (as opposed to 10 for the calculations shown here), the 1DT result was significantly different from the other three. We have not yet worked out a good way to understand or work around these effects; it is important to be careful when choosing parameters for RQA and to run experiments using several different values.

The obvious next step, on which we are currently working, is to perform RQA analyses on dynamic data sets from systems whose known dimension is greater than three. Similar results on such a data set would further strengthen our hypothesis that in order to perform RQA on a data set one need *not* first perform any delay-coordinate embedding.

IV. SUMMARY

The recurrence plot, a two-dimensional representation of a scalar time series that brings out recurrences in a very natural way, has several features that make it a uniquely powerful time-series analysis technique. It has previously been established that RPs do not require data sets to be stationary. In this paper, we present evidence that recurrence plots of data from relatively low-dimensional ($d \leqslant 3$) systems appear to be, for practical purposes, largely independent of embedding dimension. Specifically, we have demonstrated that the recurrence quantification analysis (RQA) of Trulla *et al.*,[4] a statistical, quantitative RP analysis method, does not require that data first be embedded. That is, for the purpose of finding bifurcation points in the data sets examined here, $d_E = 1$ is adequate for computing RQA statistics. We showed this by repeating the numerical experiments reported in Ref. 4, verifying that RQA statistics can detect bifurcations in a dynamically varying logistic-map time series, and then we demonstrated that those results do not actually depend on embedding dimension. We then extended this analysis to the Lorenz system, reinforcing the hypothesis that $d_E = 1$ RQA results are sufficient and that one need not embed time-series data before performing RQA.

Qualitative features of RPs also appear to remain largely unchanged with varying embedding dimension. The RPs of

experimental data from a driven pendulum, for instance, exhibit only a slight lightening with increasing embedding dimension—a secondary effect of the norms involved. The ultimate goal of this line of research is to understand this invariance of RP structure and work out useful, formalized analysis methods that can be used to study that structure. Purely quantitative analyses like RQA are a good first step along this path, but because of their lumped statistical nature, they cannot capture the details of the spatiotemporal dynamics of a time series. The structural analysis tools that we hope to develop, which will be based in theory and verified in experiment, will allow one to systematically and reliably classify the qualitative structure of these intriguing plots. In particular, we are focusing on methods that exploit pattern recognition techniques to identify and classify the topological features of RPs. A useful focus for such methods is the set of *unstable periodic orbits* (UPOs) embedded within a chaotic attractor, a set of dynamical invariants that can be used to classify such an attractor.[14] Preliminary results suggest that the set of UPOs does indeed form a basis for the gross structure (the ''skeleton'') of the recurrence plot of a chaotic attractor.

There are a variety of other rich and compelling research directions that stem from this work. The first and most obvious next step, currently underway in our group, is to test the ''RPs are independent of d_E'' hypothesis on higher-dimensional systems, such as the Mackey–Glass delay-differential equations. It would also be useful and interesting to run similar experiments and comparisons on *physical* data from systems (e.g., biological or physiological) that are thought to be nonstationary and high dimensional. The efficacy of any time-series analysis tool, including recurrence plots, depends upon the sampling frequency. The specific ways in which sampling rate affects the qualitative and quantitative nature of a RP have yet to be explored.

Almost all of the discussion in this paper concerns the embedding dimension d_E; very little focuses on the delay τ. The reason for this is that the latter is easier to deal with: the requirements on τ for a correct embedding are generally considered to be less stringent than those on d_E, and the effects of changing delay on the reconstructed dynamics are easier to understand. In theory, that is, for an infinite amount of noise-free data, any $\tau>0$ is adequate.[8] In practice, however, finite data and uncertain noise content, combined with finite-precision arithmetic, requires that the delay be large enough so that the reconstructed dynamics do not appear (with respect to machine ϵ) to have been collapsed onto a diagonal line. In the work described here, we attempt to avoid false recurrences and mitigate other numerical effects of thin-band reconstructions by choosing both threshold corridors and time delays intelligently. In particular, we use the average mutual information heuristic of Fraser and Swinney[10] to estimate τ for the pendulum data. Estimation of τ for dynamic data sets like those described in Secs. III A and B, however, is problematic; because they are nonstationary, the standard τ-estimation methods do not apply. For the logistic map data set, we chose the value used in Ref. 4 ($\tau=1$) because the goal was to duplicate and then extend those results. In the case of the Lorenz data set, we used several different values of time delay and compared the results, obtaining similar values for all, and then chose one ($\tau=0.1$) in the middle of the range to use for the analyses and plots in this paper. Finally, recall that one-embeddings do not depend in any way upon τ, so the fact that the $d_E=1$ RQA results are good bifurcation indicators strongly supports our main hypothesis.

The evidence presented in this paper to support the hypothesis that aspects of RP structure are independent of embedding dimension is highly suggestive, but certainly not definitive, and further verification and study are desperately needed. The motivation is obvious; it is not only interesting but also important to determine when, why, and how recurrence-plot analysis can avoid the considerable difficulties and often-hazy heuristics that inform the delay-coordinate embedding process. Of course, the difficulties that are inherent to recurrence-plot analysis itself will remain, but the overall data analysis process will have been simplified significantly.

ACKNOWLEDGMENTS

The authors would like to thank J. Zbilut and the *Chaos* reviewers for helpful comments. JSI was supported by a NSF Mathematical Sciences Graduate Research Traineeship No. DMS-925-6335. EB was supported by NSF NYI No. CCR-9357740, NSF No. MIP-9403223, ONR No. N00014-96-1-0720, and a Packard Fellowship in Science and Engineering from the David and Lucile Packard Foundation.

[1] J.-P. Eckmann, S. Kamphorst, and D. Ruelle, ''Recurrence plots of dynamical systems,'' Europhys. Lett. **4**, 973–977 (1987).
[2] C. Webber and J. Zbilut, ''Dynamical assessment of physiological systems and states using recurrence plot strategies,'' J. Appl. Physiol. **76**, 965–973 (1994).
[3] P. Kaluzny and R. Tarnecki, ''Recurrence plots of neural spike trains,'' Biol. Cybern. **68**, 527–534 (1993).
[4] L. Trulla, A. Giuliani, J. Zbilut, and C. Webber, ''Recurrence quantification analysis of the logistic equation with transients,'' Phys. Lett. A **223**, 255–260 (1996).
[5] M. Casdagli, ''Recurrence plots revisited,'' Physica D **108**, 12–44 (1997).
[6] T. Sauer, J. A. Yorke, and M. Casdagli, ''Embedology,'' J. Stat. Phys. **65**, 579–616 (1991).
[7] N. Packard, J. Crutchfield, J. Farmer, and R. Shaw, ''Geometry from a time series,'' Phys. Rev. Lett. **45**, 712 (1980).
[8] F. Takens, ''Detecting strange attractors in fluid turbulence,'' in *Dynamical Systems and Turbulence*, edited by D. Rand and L.-S. Young (Springer, Berlin, 1981), pp. 366–381.
[9] H. D. I. Abarbanel, *Analysis of Observed Chaotic Data* (Springer, New York, 1995).
[10] A. M. Fraser and H. L. Swinney, ''Independent coordinates for strange attractors from mutual information,'' Phys. Rev. A **33**(2), 1134–1140 (1986).
[11] M. B. Kennel, R. Brown, and H. D. I. Abarbanel, ''Determining minimum embedding dimension using a geometrical construction,'' Phys. Rev. A **45**, 3403–3411 (1992).
[12] D. Kaplan and L. Glass, *Understanding Nonlinear Dynamics* (Springer-Verlag, New York, 1995).
[13] C. E. Shannon, *The Mathematical Theory of Communication* (University of Illinois, Urbana, IL, 1964).
[14] G. H. Gunaratne, P. S. Linsay, and M. J. Vinson, ''Chaos beyond onset: A comparison of theory and experiment,'' Phys. Rev. Lett. **63**, 1 (1989).
[15] C. Sparrow, ''The Lorenz equations,'' in *Synergetics: A Workshop*, edited by H. Haken (Springer Verlag, New York, 1977), pp. 111–134.
[16] S. H. Strogatz, *Nonlinear Dynamics and Chaos* (Addison-Wesley, Reading, MA, 1994).